FULL PAPER

Appropriate reduction of the fragmentation level of subfield sequences to improve the accuracy of field delivery in IMRT for nasopharyngeal carcinoma

[1,2]YANZE SUN, [1,2]GANG ZHOU, [1,2]YAQUN ZHU, [1,2]LI ZOU and [1,2]YE TIAN

[1]Department of Radiotherapy and Oncology, The Second Affiliated Hospital of Soochow University, Suzhou, China
[2]Institute of Radiotherapy and Oncology, Soochow University, Suzhou, China

Address correspondence to: Dr Gang Zhou
E-mail: *zhougang0626@163.com*

Objective: Due to the influence of gravity, inertia and friction, there will be deviation between the position of multileaf collimator (MLC) in the delivered field and the initial intensity modulated radiotherapy (IMRT) plan. This study explores the effects of the fragmentation level of subfield sequences on this deviation and seeks ways to improve the accuracy of field delivery in IMRT for nasopharyngeal carcinoma (NPC).

Methods: 30 patients with NPC were selected, and two groups (groups A and B) of IMRT plans were made in Pinnacle planning system. Different planning parameters were used for optimization so that the subfield sequence fragmentation level of Group B was significantly lower than that of Group A. With the MapCheck2, verification plan was implemented in two ways: 0° gantry angle and the actual treatment angle, then the differences between the two verification results of each group plan were analyzed.

Results: The γ-passing rate verified at the actual treatment angle was lower than that of 0° gantry angle for each group plan, whereas the Group B plan shows small reduction. Mean change value (Δ) was decreased from 1.01% (Group A) to 0.40% (Group B) with 3%/3 mm

criteria and 2.88% (Group A) to 1.52% (Group B) with 2%/2 mm criteria, respectively. The smaller the difference (Δ), the actual output dose of the field is more consistent with the original plan. There was no significant correlation between this change and the angle of the field.

Conclusion: Appropriately reducing the fragmentation level of subfield sequence can reduce the effect of field angle on MLC position and improve the delivery accuracy of IMRT plan.

Advances in knowledge: The fragmentation level of the subfield sequence may have an impact on the accuracy of the delivery of the plan. This study demonstrates this assumption by comparing the differences between 0° and actual angle verification. Mean change value (Δ) was decreased from Group A to Group B. The smaller the difference (Δ), the actual output dose of the field is more consistent with the original plan. The result of this study may help us to understand that appropriately increasing the subfield area and reducing the fragmentation level of the subfield sequence can reduce the difference between the two verification results, which can further improve the accuracy of the plan delivery in IMRT and tumor treatment.

INTRODUCTION

Intensity modulated radiotherapy (IMRT) has become a routine technique for radiotherapy of nasopharyngeal carcinoma (NPC) because of its complex anatomy and the presence of many critical organs close to the tumor target.[1,2] IMRT uses MLC to form multiple subfields of different shapes to adjust the intensity distribution of the field to increase the dose conformity of the tumor target volume and reduce the dose of surrounding normal tissue.[3] However, because of the influence of many uncertainties in the process of treatment, there will be a position deviation of multileaf collimator (MLC) between the delivered field

and the results of the treatment plan, and it is often necessary to set tolerable errors in order to effectively delivery the field in the clinic. Therefore, the actual output dose of the field is different from the dose received by patients in the initial plan, and the dose distribution of the IMRT plan needs to be validated before treatment.[4,5]

In the actual clinical application, a two-dimensional detector matrix is commonly used at 0° gantry angle or treatment angle for measurement verification.[6,7] The 0° gantry angle can detect dose errors generated by factors such as accelerator data modeling, treatment planning

system dose algorithms, and plan data transmission.[8] However, the actual treatment angle can not only detect dose errors generated by these factors, but also by factors such as gravity, inertia, and friction, which are related to the angle of the gantry.[9–12] The difference between the results of these two verification methods reflects the influence of these factors related to the gantry angle. The smaller the difference, the actual output dose of the field is more consistent with the original plan.

In order to find the degree of difference, we designed two groups of NPC IMRT plans with different fragmentation in the subfield sequence, and then performed dose verification of the radiation field using 0° gantry angle and the actual treatment angles, and compared the difference between the two verification results.

METHODS AND MATERIALS

Patient selection and contouring

30 patients diagnosed with NPC receiving radiotherapy in our department between January 2017 and September 2017 were consecutively selected into the study. All patients were positioned and immobilized from the head to the shoulder by a thermoplastic mask. CT with a 3 mm slice thickness of the head and neck region was obtained, and imported to the treatment planning system. The physician contoured the target volume and the organs at risk (OARs) for all patients. The target volume included PTVnx, PTVnd, PTV1 and PTV2, which consisted of a 3 mm margin in all directions around GTVnx, GTVnd, CTV1, and CTV2, respectively. GTVnx and GTVnd were included the CTV1 and CTV2. The GTVnx and GTVnd covered the visible primary tumor and neck metastasis lymph nodes shown on the CT/MRI image. The CTV1 encompassed high-risk structures surrounding primary tumor and high-risk neck region, and the CTV2 encompassed low-risk neck region. The OARs included the brain stem, spinal cord, parotid glands, lenses, eyes, optic nerves, chiasm, cochlea, mandible, oral cavity, and larynx.

The prescribed dose and treatment planning

The prescribed dose included four levels: 70 Gy to the PTVnx, 66 Gy to the PTVnd, 60 Gy to the PTV1, and 54 Gy to the PTV2 in 30 fractions. The treatment goals were that prescribed dose would cover 95% of the PTV, and the maximum dose would not exceed 110%. Plan quality was evaluated using the following parameters: dose–volume histograms (DVH) analysis of targets and OAR, planning target volume (PTV) and OAR volumes and relationships, plan conformity, plan homogeneity. The dose to normal tissues was minimized within a reasonable range without affecting the target coverage (Table 1).

For this study, clinical IMRT plans were generated using DMPO module in the Pinnacle (v. 9.8; Philips) TPS, which used collapsed cone convolution (CCC) algorithm. The dose calculated grid is 3 mm. As for DMPO, the planner can preset the minimum segment area (MSA) and the minimum number of monitor units (MUs) per segment. The treatment plan with a coplanar 8-field gantry arrangement and the beam angle was distributed as much as possible on the left and right sides. 30 patients with a total of 240 fields. The distribution of all fields with an interval of 30° in the 0° to 360° range and average two fields per angle.

Table 1. Planning objectives for organs at risk

Organs at risk	Dose constrain
Brain stem	Max dose <54 Gy
Spinal cord	Max dose <54 Gy
Parotid glands	V30 <50% (at least one side)
Eyes	Max dose <50 Gy
Optic nerves	Max dose <54 Gy
Lenses	Max dose <9 Gy
Cochleas	Mean dose <45 Gy or V55 <5%
Larynx	Mean dose <45 Gy

max, maximum.

Two plans (Group A and Group B) were made for every patient according to the optimization conditions of the field parameters. For Group A, the maximum number of segments was set to 80, the minimum segment area was 5 cm², and the minimum MU was 5. For Group B, the maximum number of segments was set to 60, the minimum segment area was 8 cm², and the minimum MU was 8. A total of 60 treatment plans were designed and delivered on an Elekta Synergy Linac equipped with an 80-leaf MLC. In the preliminary pre-experiment, we made several plans with different parameters and found that if the area of the subfield is too large, such as (60, 10, 10), it will affect the quality of the plan and increase the difficulty of planning. If the area of the subfield is too small, such as (60, 7, 7) or (60, 6, 6), the experimental results are not obvious and it will not achieve the reduction of fragmentation degree of the subfield. Therefore, the Group B parameter are selected moderately. Group A (80, area 5, MU 5) is determined by the experience of the large cancer research center. At present, the general parameter setting of our radiotherapy department for NPC plan is 70–80, area 5, MU 5.

There are inherent difference in the level of complexity in the two groups of plans. Therefore, in order to evaluate the difference between groups A and B, the modulation complexity score (MCS) values were used. The MCS incorporates information about variability in leaf positions, degree of irregularity in field shape, segment weight, area, the leaf sequence variability and the aperture area variability. The subfield information of each plan was exported by the written script language, and then use MATLAB to calculate the final MCS scores according to the specific formula proposed by McNiven NL et al.[13] The MCS score ringing from 0 to 1.0, a smaller MCS score indicates a more complex plan.

MLC positional accuracy evaluation

The Picket Fence was performed on a radiochromic film. The GAFCHROMICTM RTQA2 film was used to check the position accuracy of MLC, confirm and adjust the position error of the MLC leaf. The solid water phantom with 30 x 30 cm was scaned by CT, the image was transmitted to the treatment planning system to create 11 narrow fields, each fence field was 30 cm in length, 0.6 cm in width, and the distance between the strips was 2 cm. Fix the four corners of the film with tape and cover it with a 2.0 cm solid phantom board to meet the electronic balance of the

Figure 1. Scheme of the experimental setup.
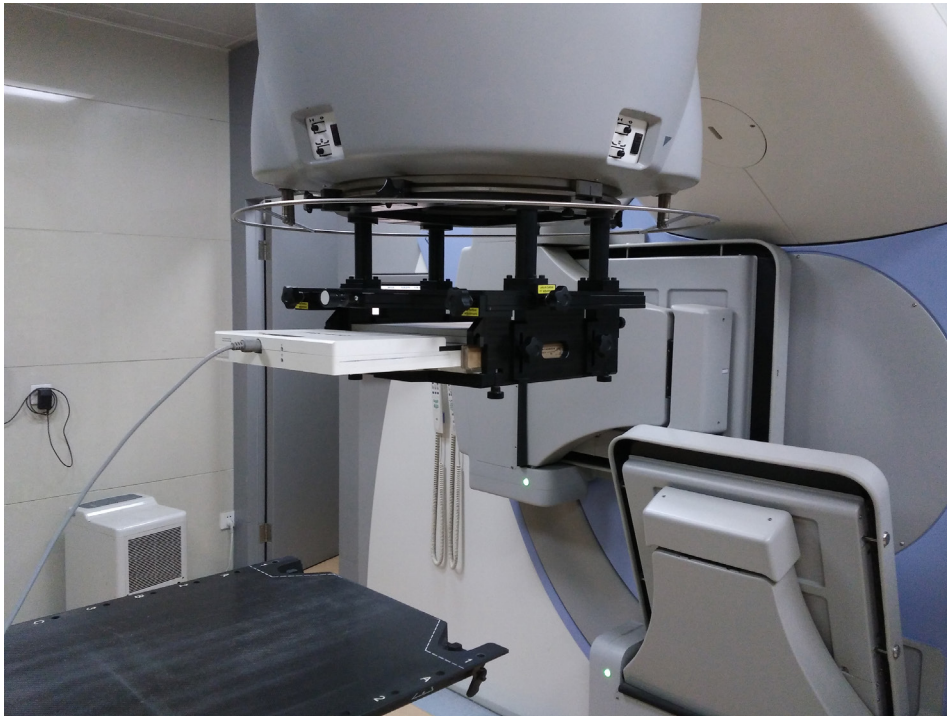
film at the maximum dose point. The film was placed on the solid phantom with a source-to-film distance (SFD) of 100 cm and the solid phantom is irradiated according to the radiation treatment plan with 250 MUs per field, following with a further analysis of the radiation width and its deviation from the nominal width.

Fixing and calibration of two-dimensional detector array

The two-dimensional detector matrix (MapCheck2) is mounted on gantry through a fixed device (Figure 1). A 2 cm solid equivalent water phantom is placed on the detector surface and fixed. After calibrating the detector for uniformity and absolute dosimetry, we irradiate every 30° using a standard 20×20 cm square field, and calculate the radiometric boundary (X direction and Y direction) maximum offset to verify the stability of the fixture.

Verification of field dose at 0° gantry angle and the treatment angle

The above device was used to verify the dose of radiation plan field at 0° gantry angle and the treatment angle. The dose distribution calculated by the treatment plan system was taken as a reference and compared with the dose results measured by the two methods, 0° gantry angle and the treatment angle, respectively. We use the γ passing rate (3%/3 mm and 2%/2 mm criteria) method to evaluate the verification results. Additionally, the local γ passing rate analysis with the dose threshold was set at 10% and the Van Dyk difference, along with the measurement uncertainty capability of the Sun Nuclear software, was used. Formula 1 is applied to calculate the difference in each field using the two ways of verification. The M in the formula is the γ-passing rate verified by the 0° angle, and N is the γ-passing rate verified by the treatment angle.

$$\Delta = | \left(M - N \right) /M \times 100\% | \qquad (1)$$

Statistical analysis

SPSS v. 19.0 software (SPSS Inc., Chicago, IL) was used for statistical analysis. The paired sample *t*-test was used to analyze the results of the two verification methods. The two-sided $p < 0.05$ was considered to be statistically significant for all tests.

RESULTS

Plan quality evaluation

Table 2 shows a full description of the data collected. Plan conformity was measured by: conformity index (CI)[14]: CI=((TV$_{95\%}$/ TV*(TV$_{95\%}$/V$_{95\%}$))). Plan homogeneity was measured by: homogeneity index (HI)[15]: HI=(D$_{2\%}$-D$_{98\%}$)/D$_{50\%}$. It can be seen from Table 2 that there is no statistical difference between the Group A plan and the Group B plan, and the two group plans are similar.

The MCS scores of per beam and per treatment plan were calculated for 30 treatment plans, 240 beams. Table 3 shows the summary of plan characteristics. The MCS scores of beam and plan for Group B is slightly higher than that of Group A, shows that Group A plans are relatively complicated.

The picket fence test results of MLC

The difference of film measured and TPS planed positions of MLC leaves for each strip picket fence should be within 0.5 mm as required by IAEA. The result showed that the differences of accurately measured MLC leaf positions were all within 0.4 mm. The differences of film measured actual widths between each pair and all pairs of leaves were within 0.5 mm as required by IAEA 0.75 mm. The standard deviation of film measured actual width

Table 2. Comparison of plan quality of between Group A and Group B. (average ±standard deviation)

	Group A (80, 5, 5)	Group B (60, 8, 8)	*t* value	*p*-value
PTVnx				
V_{70Gy} (%)	95.65 ± 0.55	95.12 ± 0.30	2.912	0.082
$D_{50\%}$ (Gy)	71.59 ± 0.31	71.83 ± 0.28	−2.355	0.086
$D_{98\%}$ (Gy)	69.47 ± 0.13	69.41 ± 0.11	1.038	0.310
$D_{2\%}$ (Gy)	73.94 ± 0.66	73.41 ± 0.64	2.020	0.057
CI	0.80 ± 0.04	0.82 ± 0.03	−1.832	0.081
HI	0.06 ± 0.01	0.06 ± 0.01	1.635	0.116
PTVnd				
V_{66Gy} (%)	95.35 ± 0.55	95.22 ± 0.30	2.112	0.095
$D_{50\%}$ (Gy)	67.25 ± 0.42	67.46 ± 0.38	−2.486	0.137
$D_{98\%}$ (Gy)	65.86 ± 0.73	65.83 ± 1.23	0.384	0.724
$D_{2\%}$ (Gy)	69.22 ± 0.83	69.25 ± 0.36	−2.006	0.315
CI	0.88 ± 0.05	0.87 ± 0.08	1.210	0.083
HI	0.07 ± 0.01	0.07 ± 0.01	1.135	0.112
PTV1				
V_{60Gy} (%)	95.03 ± 0.32	94.97 ± 0.43	2.360	0.081
$D_{50\%}$ (Gy)	61.17 ± 0.37	61.74 ± 0.27	4.408	0.230
$D_{98\%}$ (Gy)	59.97 ± 0.71	59.06 ± 0.79	2.032	0.076
$D_{2\%}$ (Gy)	63.17 ± 0.82	63.41 ± 0.57	−3.152	0.125
CI	0.78 ± 0.03	0.79 ± 0.02	3.432	0.023
HI	0.13 ± 0.02	0.11 ± 0.02	1.961	0.121
PTV2				
V_{54Gy} (%)	95.42 ± 0.65	95.38 ± 0.55	2.130	0.087
$D_{50\%}$ (Gy)	55.52 ± 4.07	55.37 ± 4.10	0.069	0.945
$D_{98\%}$ (Gy)	53.26 ± 0.65	53.16 ± 0.67	0.383	0.705
$D_{2\%}$ (Gy)	57.11 ± 1.15	57.11 ± 1.56	1.784	0.088
CI	0.86 ± 0.03	0.85 ± 0.02	1.220	0.085
HI	0.14 ± 0.03	0.13 ± 0.03	1.216	0.237

CI, conformity index; $D_{2\%}$, dose to 2% of the volume; $D_{50\%}$, dose to 50% of the volume; $D_{98\%}$, dose to 98% of the volume; HI, homogeneity index; V_{Gy}, volume receiving 100% prescription dose.

of MLC leaf between each pair and all pairs were ≤0.15 mm as required by IAEA 0.3 mm. MLC position accuracy meets experimental conditions and clinical requirements.

Test results of stability of fixtures
Table 4 shows that the distance from the center of the MapCheck to the 50% isodose line in each direction as the gantry rotated.

Table 3. Summary of plan characteristics for plans included MU and MCS scores

	Number of segments (range)	MU per beam (range)	Total MU (average)	MCS per beam (range)	Plan MCS (average)
Group A (80, 5, 5)	73–80	56–253	872	0.0893–0.2423	0.1682
Group B (60, 8, 8)	54–60	49–228	710	0.1662–0.4239	0.2071

MCS, modulation complexity score; MU, monitor unit.

Table 4. The distance from the center of the MapCheck to the 50% isodose line in each direction

	X1(cm)	Δ(cm)	X2(cm)	Δ(cm)	Y1(cm)	Δ(cm)	Y2(cm)	Δ(cm)
0°	7.784	— —	−7.757	— —	7.776	— —	−7.768	— —
30°	7.778	−0.006	−7.766	−0.009	7.784	0.008	−7.778	−0.010
60°	7.779	−0.005	−7.769	−0.012	7.780	0.004	−7.757	0.011
90°	7.786	0.002	−7.757	0.000	7.779	0.003	−7.782	−0.014
120°	7.780	−0.004	−7.770	−0.013	7.782	0.006	−7.783	−0.015
150°	7.781	−0.003	−7.771	−0.014	7.782	0.006	−7.783	−0.015
180°	7.782	−0.002	−7.771	−0.014	7.781	0.005	−7.78	−0.012
210°	7.782	−0.002	−7.774	−0.017	7.780	0.004	−7.775	−0.007
240°	7.781	−0.003	−7.771	−0.014	7.779	0.003	−7.778	−0.010
270°	7.780	−0.004	−7.769	−0.012	7.783	0.007	−7.779	−0.011
300°	7.779	−0.005	−7.769	−0.012	7.778	0.002	−7.776	−0.008
330°	7.778	−0.006	−7.770	−0.013	7.781	0.005	−7.772	−0.004

Δ indicates the difference between other angles and 0°.

With 50% of the central dose as the field boundary, the deviations of the X-axis and Y-axis field boundaries between the other gantry angles and the 0° gantry angle were calculated. The maximum offset is less than 0.5 mm. The deviation results show that the fixed device of the detector has good stability.

Verification results of field dose at 0° angle and the treatment angle

Table 5 shows the comparison of the γ passing rates of 240 fields in the Group A using 0° gantry angle and the treatment angle verification method. The results show that with the 3%/3 mm criterion, the mean γ passing rate for 0° gantry angle and the treatment angle verification were 97.63 and 96.64%, respectively, and the mean value of Δ is 1.01%. Except for 0°, 270°, 300°, and 330°, the difference was statistically significant ($p < 0.05$). With the 2%/2 mm criterion, the mean γ passing rates for 0° gantry angle and the treatment angle verification were 86.29 and 83.81%, respectively, and the mean value of Δ is 2.88%. Except for 0° and 300°, the difference was statistically significant ($p < 0.05$). Table 6 shows the results of the comparison for Group B. The mean γ passing rate for 0° gantry angle and the treatment angle verification were 97.82 and 97.40% with the 3%/3 mm criterion, respectively, and the mean value of Δ is 0.43%. The difference was not statistically significant ($p < 0.05$) except for 300°. With the 2%/2 mm criterion, the mean γ passing rates for 0° gantry angle and the treatment angle verification were 86.21 and 84.90%, respectively, and the mean value of Δ is 1.52%. The difference was not statistically significant ($p < 0.05$) except for 210°, 240°, 270°, and 300°. Compared to Group A plan, the physical treatment plan parameters in Group B made higher γ passing rate on average over actual treatment angles (97.40% *vs* 96.64% with 3%/3 mm, 84.9 *vs* 83.8% with 2%/2 mm criterion).

The relation between verification results and treatment field angle value

In Figures 2, A and B show the Δ at each treatment angle for plans of group A with 3%/3 mm and 2%/2 mm criteria, respectively.

They show that there are large differences at angles of 60°, 90°, 120°, and 150°, and the maximum difference values occur at 90°, which are 2.17 and 6.16%, respectively. C and D show the Δ at each treatment angle for plans of group B with 3%/3 mm and 2%/2 mm criteria, respectively. The larger differences occur at 210°, 240°, 270°, and 300°. The maximum difference in the C diagram is 0.77%, appearing at 300°, and the maximum difference in the D diagram is 3.35%, appearing at 240°.

DISCUSSION

When the field in the IMRT plan is delivered at its treatment angle, the accelerator will be affected by factors such as gravity, inertia, and friction.[16] These factors contribute to the deviation between the actual location of MLC and the original plan results, which are important factors affecting the delivery accuracy of the treatment plan. It is often necessary to set the tolerance error to accept this part of the effect, otherwise the field will not be able to delivery. The difference between the verification results at zero 0° angle and those at treatment angles can reflect this part of the effect. Reducing this effect will improve the consistency between the delivered field and the planned field, and reduce the dose delivery error which the planning system is unable to simulate.[17,18]

MapCheck2 is a new generation of two-dimensional semiconductor matrix with high sensitivity and resolution.[19] Buonamici and Jursinic et al pointed out that a two-dimensional semiconductor matrix can replace the film and ionization chamber for IMRT dose verification.[20,21] In this study, the MapCheck2 fixed on the accelerator gantry not only can verify the dose of field with 0° gantry angle but also the actual treatment angles, and the detector matrix panel is always perpendicular to the incident direction of the rays during the irradiation. We know that the dose distribution calculated by the treatment planning system is used as a reference, compared to the measured at treatment angle. The results show that verification in the IMRT of NPC, γ passing rate at treatment angle is lower than 0° gantry angle for non-zero gantry angle field. This conclusion is similar to the results reported by Hussein and

Table 5. Comparison of the average γ passing rate (average ± standard deviation) for zero-angle and actual-angle verification for treatment plans of Group A

Gantry angle	3%/3 mm				2%/2 mm			
	Zero-angle (%)	Treatment-angle (%)	Δ(%)	P	Zero-angle %()	Treatment-angle (%)	Δ(%)	P
0	98.29 ± 0.87	98.13 ± 0.34	0.16	0.223	87.77 ± 1.69	86.97 ± 1.48	0.91	0.074
30	96.79 ± 0.98	95.88 ± 1.13	0.94	0.003	84.21 ± 2.12	82.48 ± 2.32	2.05	0.000
60	97.93 ± 0.75	96.11 ± 0.84	1.86	0.000	84.87 ± 2.14	81.93 ± 2.79	3.43	0.000
90	96.94 ± 1.06	94.84 ± 0.92	2.17	0.000	86.49 ± 2.20	81.16 ± 2.15	6.16	0.000
120	97.73 ± 1.07	96.38 ± 1.19	1.38	0.000	87.00 ± 2.48	82.55 ± 2.32	5.11	0.000
150	98.14 ± 0.86	96.83 ± 0.83	1.33	0.000	86.71 ± 2.30	83.84 ± 2.08	3.31	0.000
180	98.03 ± 0.73	97.36 ± 0.65	0.68	0.000	88.04 ± 2.15	85.08 ± 2.34	3.36	0.000
210	97.91 ± 0.62	97.21 ± 0.67	0.71	0.001	86.94 ± 2.30	84.56 ± 2.53	2.74	0.000
240	97.91 ± 0.71	97.41 ± 0.78	0.51	0.007	86.79 ± 1.79	85.32 ± 1.63	1.69	0.019
270	97.14 ± 0.84	96.66 ± 0.81	0.49	0.132	86.78 ± 1.75	85.14 ± 2.16	1.89	0.005
300	97.37 ± 0.73	96.04 ± 0.56	1.37	0.867	84.89 ± 2.11	83.22 ± 2.15	1.97	0.850
330	97.41 ± 0.61	96.88 ± 0.77	0.54	0.082	85.03 ± 2.04	83.43 ± 2.16	1.88	0.007

Table 6. Comparison of the average γ passing rate (average ±standard deviation) for zero-angle and actual-angle verification for treatment plans of Group B

Gantry angle	3%/3 mm				2%/2 mm			
	Zero-angle (%)	Treatment-angle (%)	Δ(%)	P	Zero-angle (%)	Treatment-angle (%)	Δ(%)	P
0	97.62 ± 0.78	97.63 ± 0.95	0.01	0.959	84.96 ± 1.64	84.72 ± 1.37	0.28	0.643
30	96.67 ± 1.09	96.27 ± 1.21	0.04	0.273	83.54 ± 2.15	83.47 ± 2.03	0.08	0.911
60	98.17 ± 0.65	98.02 ± 0.96	0.15	0.639	86.74 ± 1.01	86.56 ± 1.05	0.21	0.603
90	97.62 ± 1.02	96.92 ± 1.16	0.72	0.052	87.46 ± 2.23	86.37 ± 2.11	1.25	0.089
120	97.46 ± 1.34	97.48 ± 1.21	0.02	0.199	86.82 ± 2.37	85.86 ± 2.08	1.11	0.077
150	97.81 ± 0.88	97.48 ± 0.91	0.34	0.319	85.61 ± 1.54	84.78 ± 1.68	0.97	0.197
180	98.52 ± 0.57	98.04 ± 0.79	0.49	0.058	87.13 ± 1.87	86.09 ± 2.13	1.19	0.093
210	98.19 ± 0.72	97.75 ± 0.83	0.45	0.082	87.37 ± 1.91	84.69 ± 2.26	3.07	0.000
240	98.04 ± 0.81	97.48 ± 0.44	0.57	0.052	87.51 ± 1.61	84.58 ± 1.92	3.35	0.000
270	97.99 ± 0.63	97.28 ± 0.96	0.72	0.091	87.24 ± 1.20	85.00 ± 1.39	2.57	0.000
300	98.31 ± 0.76	97.55 ± 0.82	0.77	0.009	87.13 ± 1.94	84.41 ± 2.35	3.12	0.000
330	97.38 ± 0.87	96.84 ± 0.81	0.55	0.109	83.05 ± 1.18	82.22 ± 1.76	1.00	0.387

Figure 2. Δ value is plotted for each gantry angle. (A) and (B) show the distribution of difference of the two verification results at each angle for the treatment plans of group A with 3%/3 mm and 2%/2 mm criteria, respectively. (C) and (D) show the difference at each angle for treatment plans of group B with 3%/3 mm and 2%/2 mm criteria, respectively.
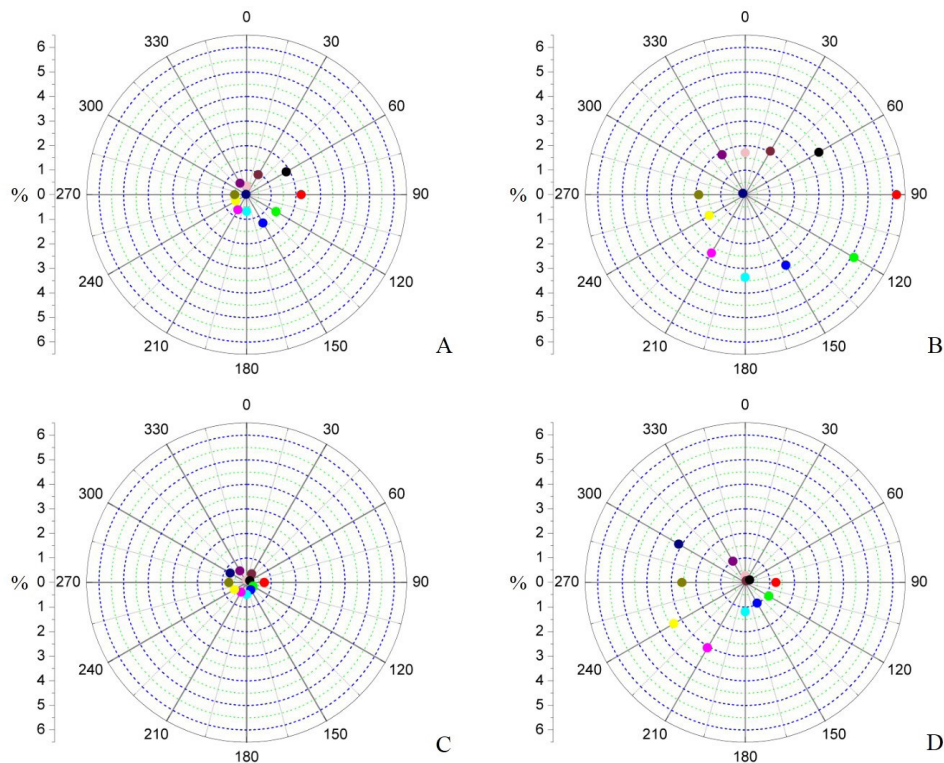
Li.[22,23] Further comparing the differences between the two verification results, we found that in the optimization results with the field parameters of Group A for IMRT of NPC, the differences between these two validation results were 1.01 and 2.88%, when the 3%/3 mm and 2%/2 mm criteria were used, respectively, and the difference was statistically significant in most of the gantry angles. This indicates that there is a relatively large decrease in the γ passing rate of the field when the treatment angle is delivered. When using group B conditions to optimize the treatment plan, the differences between these two validation results were 0.40 and 1.52% when the 3%/3 mm and 2%/2 mm criteria were used, respectively, and the difference is not statistically significant at most gantry angles. This indicates that the effect of the treatment angle on dose distribution of field is reduced. When the number of subfields in IMRT is too large, the area of the subfields and the MU is too small, which means the fragmentation level of the subfield sequences increases, leading to more dose uncertainly.[24] Giorgia et al found that the agreement between planned and delivered doses decreased as complexity of treatment plan increased.[25]

This proposed method does have certain limitations. In this study, we only analyzed the static intensity modulated radiotherapy and did not analyze the VMAT or sliding window plan. In addition, different planning system has different ways to limitate the number of subfields. As for DMPO of Pinnacle planning System, the planner can preset the MSA and the minimum number of MUs per segment. In the preliminary pre-experiment results, we found that the area of the subfield has a greater impact on the number and fragmentation of the subfield than MU. The effect of each parameter such

as MSA and minimum MU on verification results is not discussed separately in this article. In general, the higher complexity of the IMRT plan is related to many factors, such as a large number of MU and subfields, smaller subfield areas, and complex subfield shape.[25] In order to evaluate the difference between groups A and B, the actual treatment planned parameters are necessary as McNiven AL[13] pointed out that MCS scores are useful to know the difference. The MCS scores of Group B is slightly higher than that of Group A. The results further illustrate that Group A plan is a bit more complicated than Group B. In this article, the quality of the two group of plans is consistent, and there is no further discussion of the relationship between plan complexity and γ passing rate. Mean change value (Δ) was decreased from Group A to Group B. The smaller the difference (Δ), the actual output dose of the field is more consistent with the original plan. The result of this study may help us to understand that appropriately increasing the subfield area and reducing the fragmentation level of the subfield sequence can reduce the difference between the two verification results, which can further improve the accuracy of the plan delivery in IMRT. In addition, the results of this study show that there is no significant correlation between the effect of the treatment angle on dose distribution and the angle value of the field. That means there is no particular angle value at which the difference between the two verification methods is always higher or lower. It is probably because the accelerator is affected by many factors at the treatment angle. In addition to gravity, inertia, and friction, it is also affected by the repeatability of the MLC arrival position, the calibration procedure of MLC, and the consistency of light field and radiation field, which are unrelated to the gantry angle value.

CONCLUSIONS

The machine parameters when the accelerator is delivering the field at the treatment angle is an important factor affecting the delivery accuracy of IMRT plan. The deviation between verified at actual treatment angle and the 0° gantry angle can further reflect the delivery accuracy. This effect is related to the fragmentation level of the subfield sequences. If the total number of subfields is reduced appropriately, the area of subfields is increased and the minimum MU is increased, this effect will be reduced and the delivery accuracy of IMRT will be improved.

FUNDING

REFERENCES

1. Kam MKM, Chau RMC, Suen J, Choi PHK, Teo PML. Intensity-Modulated radiotherapy in nasopharyngeal carcinoma: dosimetric advantage over conventional plans and feasibility of dose escalation. *Int J Radiat Oncol Biol Phys* 2003; **56**: 145–57. doi: https://doi.org/10.1016/s0360-3016(03)00075-0

2. Marta GN, Silva V, de Andrade Carvalho H, de Arruda FF, Hanna SA, Gadia R, et al. Intensity-Modulated radiation therapy for head and neck cancer: systematic review and meta-analysis. *Radiother Oncol* 2014; **110**: 9–15. doi: https://doi.org/10.1016/j.radonc.2013.11.010

3. Gomez-Millan J, Fernández JR, Medina Carmona JA. Current status of IMRT in head and neck cancer. *Rep Pract Oncol Radiother* 2013; **18**: 371–5. doi: https://doi.org/10.1016/j.rpor.2013.09.008

4. Klein EE, Hanley J, Bayouth J, Yin F-F, Simon W, Dresser S, et al. Task group 142 report: quality assurance of medical accelerators. *Med Phys* 2009; **36**(9Part1): 4197–212. doi: https://doi.org/10.1118/1.3190392

5. Ezzell GA, Burmeister JW, Dogan N, LoSasso TJ, Mechalakos JG, Mihailidis D, et al. Imrt commissioning: multiple institution planning and dosimetry comparisons, a report from AAPM task group 119. *Med Phys* 2009; **36**: 5359–73. doi: https://doi.org/10.1118/1.3238104

6. Low DA, Moran JM, Dempsey JF, Dong L, Oldham M. Dosimetry tools and techniques for IMRT. *Med Phys* 2011; **38**: 1313–38. doi: https://doi.org/10.1118/1.3514120

7. Nelms BE, Simon JA. A survey on planar IMRT QA analysis. *Journal of Applied Clinical Medical Physics* 2007; **8**: 76–90. doi: https://doi.org/10.1120/jacmp.v8i3.2448

8. Poppe B, Blechschmidt A, Djouguela A, Kollhoff R, Rubach A, Willborn KC, et al. Two-Dimensional ionization chamber arrays for IMRT plan verification. *Med Phys* 2006; **33**: 1005–15. doi: https://doi.org/10.1118/1.2179167

9. Bai S, Li G, Wang M, Jiang Q, Zhang Y, Wei Y, et al. Effect of Mlc leaf position, collimator rotation angle, and gantry rotation angle errors on intensity-modulated radiotherapy plans for nasopharyngeal carcinoma. *Med Dosim* 2013; **38**: 143–7. doi: https://doi.org/10.1016/j.meddos.2012.10.002

10. Nelms BE, Zhen H, Tomé WA. Per-beam, planar IMRT QA passing rates do not predict clinically relevant patient dose errors. *Med Phys* 2011; **38**: 1037–44. doi: https://doi.org/10.1118/1.3544657

11. Losasso T. Imrt delivery performance with a varian multileaf collimator. *Int J Radiat Oncol Biol Phys* 2008; **71**(1 Suppl): S85–8. doi: https://doi.org/10.1016/j.ijrobp.2007.06.082

12. Sumida I, Yamaguchi H, Kizaki H, Koizumi M, Ogata T, Takahashi Y, et al. Quality assurance of Mlc leaf position accuracy and relative dose effect at the Mlc abutment region using an electronic portal imaging device. *J Radiat Res* 2012; **53**: 798–806. doi: https://doi.org/10.1093/jrr/rrs038

13. McNiven AL, Sharpe MB, Purdie TG. A new metric for assessing IMRT modulation complexity and plan deliverability. *Med Phys* 2010; **37**: 505–15. doi: https://doi.org/10.1118/1.3276775

14. Paddick I, Lippitz B. A simple dose gradient measurement tool to complement the conformity index. *J Neurosurg* 2006; **105 Suppl**(Supplement): 194–201. doi: https://doi.org/10.3171/sup.2006.105.7.194

15. Kataria T, Sharma K, Subramani V, Karrthick KP, Bisht SS. Homogeneity index: an objective tool for assessment of conformal radiation treatments. *J Med Phys* 2012; **37**: 207–13. doi: https://doi.org/10.4103/0971-6203.103606

16. Clarke MF, Budgell GJ. Use of an amorphous silicon EpiD for measuring MLC calibration at varying gantry angle. *Phys Med Biol* 2008; **53**: 473–85. doi: https://doi.org/10.1088/0031-9155/53/2/013

17. Kerns JR, Childress N, Kry SF. *A multi-institution evaluation of Mlc log files and performance in IMRT delivery. Radiat Oncol* 2014; **9**: 176. doi: https://doi.org/10.1186/1748-717X-9-176

18. Wang Y, Pang X, Feng L, Wang H, Bai Y. Correlation between gamma passing rate and complexity of IMRT plan due to MLC position errors. *Phys Med* 2018; **47**: 112–20. doi: https://doi.org/10.1016/j.ejmp.2018.03.003

19. Rinaldin G, Perna L, Agnello G, Pallazzi G, Cattaneo GM, Fiorino C, et al. Quality assurance of rapid Arc treatments: performances and pre-clinical Verifications of a planar detector (MapCHECK2. *Phys Med* 2014; **30**: 184–90. doi: https://doi.org/10.1016/j.ejmp.2013.05.004

20. Buonamici FB, Compagnucci A, Marrazzo L, Russo S, Bucciolini M. An intercomparison between film dosimetry and diode matrix for IMRT quality assurance. *Med Phys* 2007; **34**: 1372–9. doi: https://doi.org/10.1118/1.2713426

21. Jursinic PA, Nelms BE. A 2-D diode array and analysis software for verification of intensity modulated radiation therapy delivery. *Med Phys* 2003; **30**: 870–9. doi: https://doi.org/10.1118/1.1567831

22. Hussein M, Adams EJ, Jordan TJ, Clark CH, Nisbet A, et al. A critical evaluation of the PTW 2D-array seven29 and OCTAVIUS II phantom for IMRT and VMAT verification. *Journal of Applied Clinical Medical Physics* 2013; **14**: 274–92. doi: https://doi.org/10.1120/jacmp.v14i6.4460

23. Li G, Zhang Y, Jiang X, Bai S, Peng G, Wu K, et al. Evaluation of the ArcCHECK QA system for IMRT and VMAT verification. *Phys Med* 2013; **29**: 295–303. doi: https://doi.org/10.1016/j.ejmp.2012.04.005

24. Azimi R, Alaei P, Higgins P. The effect of small field output factor measurements on IMRT dosimetry. *Med Phys* 2012; **39**: 4691–4. doi: https://doi.org/10.1118/1.4736527

25. Giorgia N, Antonella F, Eugenio V, Alessandro C, Filippo A, Luca C, et al. What is an acceptably smoothed fluence? Dosimetric and delivery considerations for dynamic sliding window IMRT. *Radiat Oncol* 2007; **2**: 42. doi: https://doi.org/10.1186/1748-717X-2-42